Cancer Letters 402 (2017) 153–165

Contents lists available at ScienceDirect

Cancer Letters

journal homepage: www.elsevier.com/locate/canlet

Original Article

RSPO2 suppresses colorectal cancer metastasis by counteracting the Wnt5a/Fzd7-driven noncanonical Wnt pathway

Xiaoming Dong [a, 1], Wanqin Liao [a, 1], Li Zhang [a, 1], Xi Tu [b], Jin Hu [a], Tianke Chen [a], Xiaowei Dai [a], Yan Xiong [a], Weicheng Liang [a], Chaodong Ding [a], Rui Liu [a], Juji Dai [a], Ouchen Wang [c], Liting Lu [a], Xincheng Lu [a, *]

[a] School of Basic Medical Sciences, Wenzhou Medical University, Wenzhou, 325000, China
[b] Department of Clinical Laboratory, Taizhou Hospital of Zhejiang Province, Zhejiang, 317000, China
[c] The First Affiliated Hospital of Wenzhou Medical University, Wenzhou, 325000, China

ARTICLE INFO

Article history:
Received 20 January 2017
Received in revised form
18 May 2017
Accepted 26 May 2017

Keywords:
RSPO2
Colorectal cancer
Metastasis
Fzd7
Wnt5a

ABSTRACT

R-spondins play critical roles in development, stem cell survival, and tumorigenicity by modulating Wnt/β-catenin signaling; however, the role of R-spondins in noncanonical Wnt signaling regulation remains largely unknown. We demonstrate here that R-spondin 2 (RSPO2) has an inhibitory effect on colorectal cancer (CRC) cell migration, invasion, and metastasis. Reduced RSPO2 expression was associated with tumor metastasis and poor survival in CRC patients. The metastasis-suppressive activity of RSPO2 was independent of the Wnt/β-catenin signaling pathway but dependent on the Fzd7-mediated noncanonical Wnt signaling pathway. The physical interaction of RSPO2 and Fzd7 increased the degradation of cell surface Fzd7 via ZNRF3-mediated ubiquitination, which led to the suppression of the downstream PKC/ERK signaling cascade. In late-stage metastatic cancer, Wnt5a promoted CRC cell migration by preventing degradation of Fzd7, and RSPO2 antagonized Wnt5a-driven noncanonical Wnt signaling activation and tumor cell migration by blocking the binding of Wnt5a to the Fzd7 receptor. Our study reveals a novel RSPO2/Wnt5a-competing noncanonical Wnt signaling mechanism that regulates cellular migration and invasion, and our data suggest that secreted RSPO2 protein could serve as a potential therapy for Wnt5a/Fzd7-driven aggressive CRC tumors.

Introduction

Human colorectal cancer (CRC) is the third most common cancer worldwide [1]. Although radical resection of non-metastatic CRC significantly increases the survival rate, metastasis remains the major cause of mortality in CRC patients [2]. CRC tumor metastasis includes a series of biological processes, and a number of molecules and pathways related to the metastatic process have been identified [3]. The Wnt signaling pathway is one of the major pathways involved in CRC metastasis. Canonical Wnt/β-catenin signaling can regulate transcription factors and cytokines, modulate epithelial-mesenchymal transition (EMT), and thereby play critical roles in CRC cell adhesion, migration, and invasion [4]. The up-regulation of noncanonical Wnt signaling, including the PKC and JNK/ERK pathways, has also been observed during colorectal cancer EMT and metastasis [5,6].

The R-spondins (RSPO) are members of a superfamily of thrombospondin type 1 repeat (TSR-1)-containing proteins that generally act as Wnt/β-catenin signaling agonists [7]. There are four structurally related, secreted proteins (RSPO1-4) in the R-spondin family, all containing two furin-like cysteine-rich domains that are necessary and sufficient for Wnt signal potentiation [8]. Accumulated studies have characterized the important roles of R-spondin proteins in a broad range of physiological and developmental processes, such as sex determination, cell proliferation, embryonic development, bone formation, and stem cell survival, which are implemented mainly through the canonical Wnt/β-catenin

Abbreviation: RSPO2, R-spondin 2; CRC, colorectal cancer; RSPO, R-spondins; TSR-1, thrombospondin type 1 repeat; LGRs, leucine-rich repeat-containing G-protein-coupled receptors; Wnt/PCP, Wnt/planar cell polarity; MAPK, mitogen-activated protein kinase; PDX, patient-derived xenograft; MMPs, matrix metalloproteases; EMT, Epithelial-mesenchymal transition; qRT-PCR, quantitative real-time PCR.

* Corresponding author. Wenzhou Medical University, 270# Xueyuanxi Road, Wenzhou, 325000, China.
E-mail address: xinchenglu@yahoo.com (X. Lu).

[1] These authors contributed equally to this work.

http://dx.doi.org/10.1016/j.canlet.2017.05.024
0304-3835/

signaling pathway [9–12]. The leucine-rich repeat-containing G protein-coupled receptors (LGR) 4–6, three closely related orphans in the LGR family, have been identified as high-affinity cell-surface receptors for R-spondin proteins [13,14]. The LGR/RSPO complex acts by neutralizing ZNRF3 and RNF43, two transmembrane E3 ligases that remove Wnt receptors from the cell surface, and thereby regulates canonical Wnt/β-catenin signaling activity [15]. In contrast to the extensive studies related to canonical Wnt/β-catenin signal transduction, little attention has been paid to the specificity of R-spondin in noncanonical Wnt signaling transduction. The interaction between RSPO3 and syndecan 4 activates Wnt/planar cell polarity (Wnt/PCP) signaling [16]; Rspo3 deletion blocks noncanonical Wnt/calcium signaling at the level of NFAT [17]; LGR4/LGR5 promotes RSPO-mediated Wnt/PCP signaling [18]. These findings suggest that R-spondin proteins have potent activity toward noncanonical Wnt signaling regulation.

The prominent influence of R-spondins on Wnt signaling suggests that they may play critical roles in human cancer initiation, growth, and metastasis. Ectopic RSPO2/3 expression in mouse mammary epithelial cells increases cell invasiveness *in vitro* and tumor formation and metastasis *in vivo* [19,20]. In a transposon-based genetic screen in mice, alteration of the RSPO2 gene is linked to CRC [21]. Furthermore, recurrent gene fusion of RSPO2 and RSPO3 occurs in prostate cancer, colon cancer, and human Schwann cell tumors [22–25]. A recent study has also indicated that RSPO3-LGR4 signaling promotes tumor metastasis in Keap1-deficient lung adenocarcinomas [26]. In contrast to the oncogenic function in mammary and prostate cancers, RSPO1 exhibits tumor suppressor activity in lymphocytic leukemia and skin carcinoma. Humans carrying RSPO1-null mutations are predisposed to skin carcinoma [27,28]. In our previous report, we demonstrated that RSPO2 suppresses CRC tumor growth through an LGR5-dependent Wnt/β-catenin signaling feedback mechanism [29]. Together, these findings suggest that R-spondins can function either as oncogenes or tumor suppressors depending on the type of cancer and/or the presence of receptors.

Previously, we reported that RSPO2 is down-regulated in the majority of CRC tumors. Moreover, the reduced RSPO2 expression in the tumors of CRC patients is associated with tumor infiltration and lymph node metastasis [29]. In this study, we evaluated the role of RSPO2 in human CRC tumor metastasis. We provide evidence that RSPO2 acts as a noncanonical Wnt signaling antagonist that inhibits EMT and metastasis in human CRC. Reduced RSPO2 expression was associated with shorter survival times in CRC patients. In addition, we performed detailed investigations to uncover the association between RSPO2 and the downstream genes/pathways that mediate metastasis in CRC tumors. Our study reveals a novel RSPO2/Wnt5a-competing noncanonical Wnt pathway that regulates the EMT, migration, and invasion of CRC cells.

Materials and methods

Tissue samples, cell lines, and antibodies

Fresh primary colorectal tumors and matched adjacent normal mucosa with appropriate Institutional Review Board approval and patient-informed consent were obtained from the First Affiliated Hospital of Wenzhou Medical University. HEK293, SW480, LOVO, and other CRC cell lines were obtained from the American Type Culture Collection (ATCC). Routine cell cultures were maintained in medium supplemented with 10% FBS and 1% penicillin/streptomycin and incubated in a 5% CO_2 atmosphere at 37 °C. Experiments with exogenous RSPO2 protein stimulation, RSPO2 overexpression, or si-RSPO2 knockdown were performed in medium containing 5% FBS. The following antibodies were used: human β-catenin (#9587S), c-Myc (#5605S), CD44 (#3570S), GAPDH (#2118), JNK (#9252), phospho-JNK (Thr183/Tyr185) (#9255), p38 MAP kinase (#9212), phospho-p38 MAP Kinase (Thr180/Tyr182) (#9211), phospho-p44/42 ERK MAP kinase (Thr202/Tyr204) (#9101), p44/42 ERK MAP kinase (#9102), EGF receptor (#2232), phospho-EGF receptor (Tyr1068) (#3777), phospho-PKC (#2060), β-actin (#4970S), Myc-tag (#2278), tubulin (#2144) antibodies, and MEK inhibitor U0126 (#9903) were purchased from Cell Signaling Technology; Fzd2 (MAB1307-050) antibody and recombinant human Wnt5a and RSPO2 proteins were obtained from R&D Systems; Cetuximab was purchased from Merck (German); ZNRF3 (sc-86958), PEA3 (sc-113), Wnt5a (sc-30224), c-Jun (sc-44), c-Fos (sc-447), RSPO2 (sc-74883), TIMP1 (sc-5538), C-met (sc-10), and HA (sc-7392) antibodies were purchased from Santa Cruz Biotechnology; Fibronectin (610077), Vimentin (550513), N-cadherin (610920), and E-cadherin (610181) antibodies were purchased from BD Biosciences; Fzd7 (ab64636), MMP2 (ab80737), MMP7 (ab39984), MMP9 (ab76003), and IR-β (ab69508) antibodies were purchased from Abcam; and Ras (1862335) and Flag (TA50011) antibodies were purchased from Thermo Scientific and Origene, respectively.

Plasmids

The CD44s plasmid was a gift from Véronique Orian-Rousseau (Institute of Toxicology and Genetics, Karlsruhe Institute of Technology, Campus North, Karlsruhe, Germany). The Fzd7 plasmid was a gift from Karl Willert (Department of Cellular and Molecular Medicine, Stem Cell Program, University of California, San Diego, CA, USA). The full-length Fzd7 cDNA was further amplified by PCR and subcloned into the pcDNA3.1 vector to append a C-terminal Myc tag. The TopFlash, FopFlash, and pRL-TK plasmids were obtained from Promega. Ub-HA (HA-Ubquitin plasmid #18712) was purchased from Addgene. ZNRF3 plasmid was purchased from Origene. The full-length human RSPO2 and MMP7 cDNA were amplified from HEK293 cells using the One-Step RT-PCR System kit (Invitrogen), subcloned into pcDNA3.1 (Invitrogen), and verified by DNA sequencing.

Quantitative real-time PCR (qRT-PCR)

Total RNA was isolated from CRC cell lines and tumor samples using TRIzol reagent (Invitrogen). A total of 2 μg of total RNA was reverse-transcribed into cDNA with MLV-reverse transcriptase (Invitrogen), and each cDNA sample was analyzed in triplicate on an ABI 7300 Real-Time Detection system (Applied Biosystems) using SYBR Green (Tiangen, China) according to the manufacturer's protocol. Endogenous housekeeping genes (β-actin or GAPDH) were used as internal standards. The cycle conditions were as follows: 95 °C for 2 min followed by 40 cycles of 95 °C for 15 s, 60 °C for 30 s, and 68 °C for 30 s. The primer sequences are listed in Supplementary Table S1. The relative quantification of the mRNA was calculated using the comparative threshold cycle (Ct) method. When necessary, we converted ΔΔCt to a fold change in expression using the formula $2^{-\Delta\Delta Ct}$.

Transient and stable transfection

Transfections were performed using Lipofectamine 2000 reagent (Invitrogen) according to the manufacturer's instructions. pEGFP-N1 (Clontech) was co-transfected to assess the transfection efficiency. To obtain stable transfectants, the transfected cells were grown in medium with G418, and resistant clones were confirmed by western blotting.

β-Catenin reporter assay

The β-catenin reporter pTopFlash (100 ng) was transfected into cells cultured in 24-well plates using Lipofectamine 2000 reagent (Invitrogen). A total of 2 ng of pRL-TK (Renilla luciferase) was co-transfected as an internal control. Forty-eight hours after transfection, the cells were treated with different concentration of recombinant RSPO2 or Wnt5a protein, and luciferase activity was measured 12 h after protein addition. The luciferase reporter assay was performed using the Dual-luciferase Reporter Assay System (Promega). To control for transfection efficiency, firefly luciferase levels were normalized to Renilla luciferase levels to generate a measure of relative luciferase units. An Envision Luminometer (Perkin-Elmer) was used to detect luminescence. The experimental data are presented as the mean ± SD of three independent wells.

AP-1 reporter assay

pAP1-luc vector (Beyotime Biotechnology, Shanghai, China) (100 ng) was transfected into cells cultured in 24-well plates using Lipofectamine 2000 reagent (Invitrogen). A total of 2 ng of pRL-TK (Renilla luciferase) was co-transfected as an internal control. Forty-eight hours after transfection, the cells were treated with different concentrations of recombinant RSPO2 protein, and luciferase activity was measured 12 h after RSPO2 protein addition. The experimental data are presented as the mean ± SD of three independent wells.

Small interfering RNA

The SMARTpool siRNA reagents for RSPO2 (si-RSPO2), ZNRF3 (si-ZNRF3), Fzd7 (si-Fzd7), PEA3 (si-PEA3), CD44 (si-CD44) and non-targeting oligonucleotides were purchased from Dharmacon Research. Cells grown to a confluence of ~50% were transfected with siRNA using Lipofectamine 2000 reagent (Invitrogen) according to the manufacturer's protocol. If necessary, a second transfection was performed at 48 h, and the experiments were performed 24 h after the second transfection. The knockdown efficiency was determined by qRT-PCR or western blotting.

MTT assay and clonogenic assay

Cell viability was determined with the MTT (Sigma) assay as described previously [29]. For the clonogenic assay, a total of 500–1000 stable RSPO2-overexpressing cells were seeded in a 6-well plate and maintained for 10 days in medium containing 5% FBS. The colonies were stained with 0.1% crystal violet, and colonies with more than 50 cells were counted.

Wound-healing assay

Wound-healing assays were performed using 6-well plates. SW480 and LOVO cells stably expressing RSPO2 were seeded to confluence 24 h before the experiment. The cell layers were carefully scratched with 200-μl sterile pipette tips and washed twice with fresh medium. Cells were imaged under a light microscope at 40 × magnification power every 24 h.

Trans-well migration and invasion assay

Trans-well migration assays were performed using Corning chambers with 8-μm pore polycarbonate membrane filter inserts in 24-well plates. Cells (1×10^5) in 100 μl of serum-free medium were seeded in the upper chamber, and 600 μl of completed medium containing 10% FBS was placed in the lower chamber. After incubation for 24 h, the cells on top of the membrane were wiped off with cotton swabs, and the cells that had migrated to the bottom well were fixed in methanol for 10 min and stained with 0.05% crystal violet. Five randomly selected fields of the membrane were counted under an inverted microscope at 100 × magnification power. *Trans*-well invasion assays were performed using the same protocol as the migration assay, except that the transwell membranes were coated with 1:3 diluted Matrigel (BD Biosciences, Heidelberg, Germany) before cell seeding.

In vivo metastasis assay

Six-week-old male athymic nude mice (nu/nu) were purchased from the Vital River Experimental Animal Center (Beijing, China) and maintained under pathogen-free conditions. Cells stably transfected with the RSPO2 expression plasmid (R2) or control empty vector (Vec) were labeled with luciferase-overexpressing lentivirus before injection. Cells (1×10^6) in 100 μl of PBS were injected into the left ventricle of nude mice. A luciferin (Cold Spring Biotech Corp. China) solution (150 mg/kg) was intraperitoneally injected into mice 15 min before imaging. The metastatic lesions were monitored by luciferase expression detected with the IVIS Lumina Series III *in vivo* imaging system (Caliper Life Sciences, USA) every two weeks. At the end of the experiments (10 weeks after cell injection), the mice were sacrificed, and H&E staining was used to detect tumor metastatic nodules in lung and liver. All animals were maintained and used in accordance with the guidelines of the Institutional Animal Care and Use Committee of Wenzhou Medical University.

Gelatin zymography assay

The enzyme activities of MMP2 and MMP9 were assessed by zymography using gelatin-impregnated gels. Briefly, 20 μg of total protein frozen-concentrated from the culture medium was loaded onto 10% SDS-PAGE gels containing 0.1 g/ml gelatin (Sigma), and electrophoretically separated under non-reducing conditions. After renaturing in a mixture of 50 mM Tris pH 7.5, 0.1 M NaCl and 2.5% Triton X-100, the gels were incubated for 20 h in 50 mM Tris, 10 mM $CaCl_2$ and 0.02% NaN_3 at 37 °C. Gels were stained with Coomassie blue and destained in a mixture of 5% acetic acid and 10% methanol. MMP2 and MMP9 were identified by comparison to molecular weight standards.

Western blotting

Protein levels were determined by western blotting as described previously [29]. Briefly, cells were washed and lysed in lysis buffer supplemented with Protease/Phosphatase Inhibitor Cocktail (Cell Signaling Technology). After incubation on ice for 20 min, the lysate was centrifuged at 12,000 rpm for 20 min at 4 °C, and the supernatant was collected. To prepare cytosolic (non-membrane bound) β-catenin, cell lysates were treated with ConA-sepharose beads (Amersham) for 4 h and then centrifuged to remove the cadherin-bound β-catenin. Cell surface proteins were isolated by whole cell biotinylation and avidin agarose pull-down using the Cell Surface Protein Isolation Kit (Pierce) according to the manufacturer's instructions. Proteins were separated by SDS-PAGE and transferred to PVDF membranes (Bio-Rad). After blocking in 5% milk in TBST (0.1% Tween-20), the membranes were incubated with primary antibodies (1:500–1000) followed by HRP-conjugated secondary antibodies. Protein bands were visualized with the Immun-Star™ HRP Chemiluminescence kit (Bio-Rad).

Ras activity assay

Cells were treated without or with 100 ng/ml RSPO2 protein for 6 h and then lysed in lysis/binding buffer (25 mM Tris-HCl, pH 7.2, 150 mM NaCl, 5 mM $MgCl_2$, 1% NP40 and 5% glycerol) supplemented with Protease/Phosphatase Inhibitor Cocktail (Cell Signaling Technology). Lysates containing 1 mg of protein were used to assay Ras-GTP using the Active Ras Pull-down and detection kit (Thermo Scientific) according to the manufacturer's instructions. Products were resolved by SDS-PAGE, and western blotting with anti-Ras antibody was performed.

Immunoprecipitation

Cells were washed with ice-cold PBS and lysed in immunoprecipitation assay buffer (50 mM Tris/HCl, pH 7.5, 150 mM NaCl, 1% Triton X-100, 1 mM EDTA and 10% glycerol) supplemented with Protease/Phosphatase Inhibitor Cocktail (Cell Signaling Technology). Lysates were incubated on ice for 20 min and centrifuged at 12,000 rpm for 20 min at 4 °C. Cell lysates were incubated with the corresponding primary antibody overnight at 4 °C, followed by incubation with Protein G-sepharose (GE healthcare) for 1 h at 4 °C. The beads were washed four times with immunoprecipitation assay buffer, suspended in Laemmli buffer, and boiled for 5 min. Samples were analyzed by western blotting with the indicated antibodies.

Ubiquitination assay

Cells were transfected with the HA-Ubiquitin plasmid. Twenty-four hours after transfection, the cells were treated with 25 μM proteasome inhibitor MG132 for 4 h and then lysed in ubiquitination assay buffer (50 mM Tris/HCl, pH 7.4, 150 mM NaCl, 1 mM EDTA and 1% NP40) containing Protease/Phosphatase Inhibitor Cocktail (Cell Signaling Technology). Cell lysates were clarified and incubated with Fzd7 antibody overnight at 4 °C. Immunocomplexes were incubated with Protein G-sepharose (GE healthcare) for another 3 h at 4 °C, washed four times with wash buffer (50 mM Tris/HCl pH 7.4, 150 mM NaCl, 1 mM EDTA, 0.1% NP40), and boiled for 5 min in Laemmli buffer before separation by SDS-PAGE. Western blotting was performed with HA-tagged antibody to detect ubiquitinated Fzd7.

Immunofluorescence imaging

The immunofluorescence analysis was performed as described previously [29]. Briefly, cells were seeded on coverslips for 40 h and then stimulated with RSPO2 protein (100 ng/ml) or were unstimulated (control) for 6 h. After gentle washes with PBS, the cells were fixed with 4% formaldehyde and permeabilized with 0.5% Triton X-100 in PBS. Cells were subsequently blocked with 2% BSA in PBS-0.1% Triton X-100 followed by incubation with primary antibody (diluted 1:100) at 4 °C overnight. After three washes with PBS-0.1% Triton X-100, the samples were incubated with fluorescently labeled secondary antibodies (diluted 1:1000). Coverslips were mounted on glass slides in the presence of DAPI for nuclear staining, and cell images were recorded using a ZEISS confocal microscope.

Statistical analyses

The data represent the mean ± SD unless otherwise indicated. Statistical comparisons were performed using Student's *t*-test. Significance was considered $P < 0.05$. Kaplan-Meier survival analysis was performed using the R2 bioinformatics platform (http://r2.amc.nl). The optimal cut-off level for the categories was determined by Kaplan scanning, and the significance (log-rank test) was corrected for multiple testing (Bonferroni correction). The correlation between RSPO2 and Wnt5a expression was evaluated by calculating the Spearman rank correlation coefficient using the Statistical Package for the Social Sciences (SPSS) version 17.0.

Results

RSPO2 inhibits CRC cell migration, invasion, and metastasis

We have previously reported that reduced RSPO2 expression in CRC is associated with tumor infiltration and lymph node metastasis [29]. This finding prompted us to speculate that RSPO2 may play important roles in CRC metastasis. Indeed, we found that siRNA-mediated knockdown of RSPO2 promoted the migration and invasion of SW480 and LOVO CRC cells, as characterized by *trans*-well migration/Matrigel assays (Fig. 1A–B, Supplementary Fig. 1A). Conversely, recombinant RSPO2 protein treatment significantly reduced CRC cell migration (Fig. 1C). Stable RSPO2 overexpression in SW480 and LOVO cells also decreased CRC cell motility (Fig. 1D–E, Supplementary Fig. 1B). To examine the effects of RSPO2 *in vivo*, a bioluminescent murine model was used. SW480 control cells (SW480-Vec) and SW480 cells stably overexpressing RSPO2 (SW480-R2) were separately injected into the left ventricle of nude mice to induce experimental metastases. As shown in Fig. 1F–G, bioluminescent signals appeared in SW480 control mice within 2 weeks and progressively intensified in the following weeks. In contrast, substantially weaker bioluminescent signals and fewer metastatic lesions were detected after 4 weeks in mice that

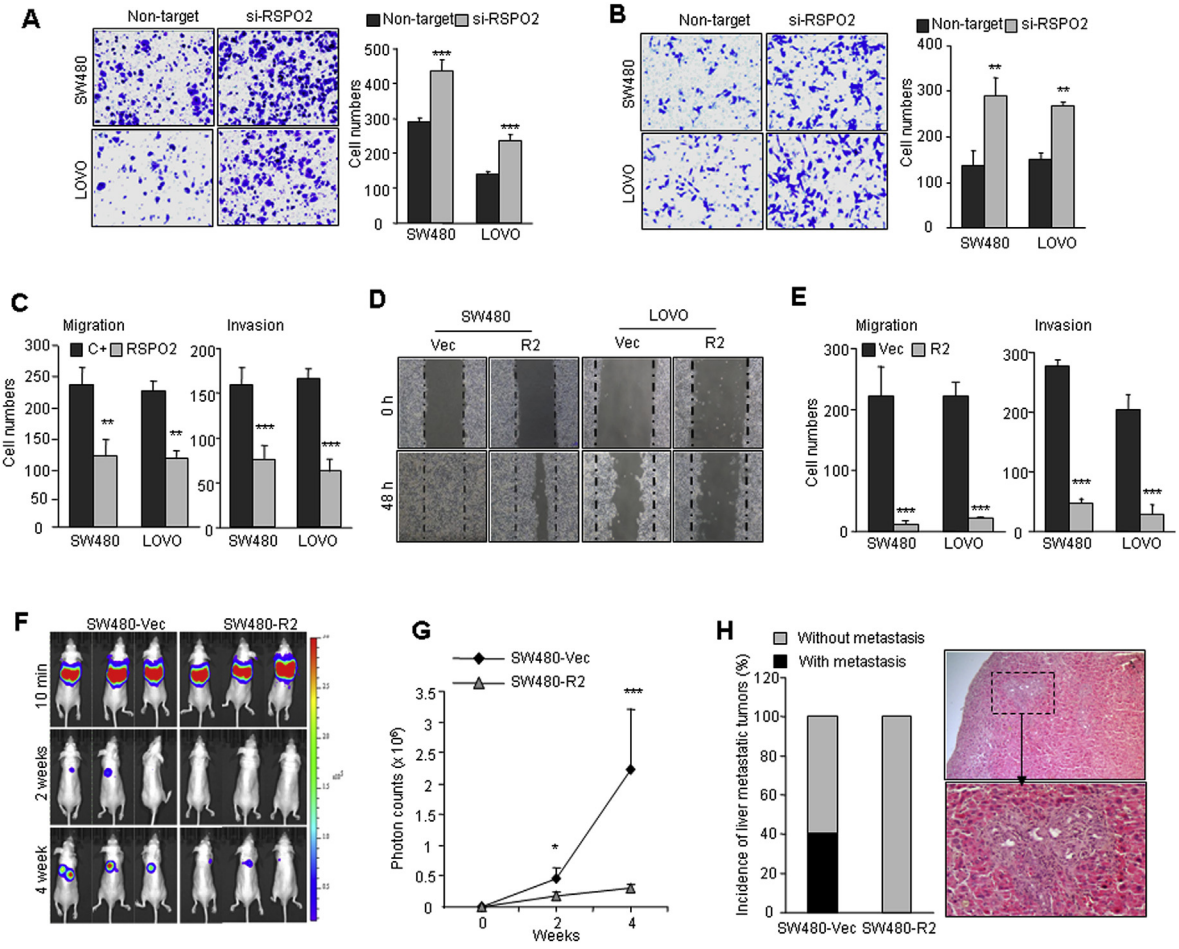

Fig. 1. RSPO2 inhibits CRC cell migration, invasion and metastasis. (**A-B**) *Trans*-well migration and invasion assays of CRC cells after siRNA-mediated RSPO2 knockdown. Non-target siRNA was used as a control. Representative images of the assay (left). The error bars indicate the SD of three independent experiments. **P < 0.01 vs. non-target; ***P < 0.001 vs. non-target. (**C**) *Trans*-well migration and invasion assays of CRC cells treated with recombinant RSPO2 protein (cells were pretreated with 100 ng/ml RSPO2 protein for 6 h). The error bars indicate the SD of three independent experiments. **P < 0.01 vs. C+ (PBS); ***P < 0.001 vs. C+. (**D**) Wound-healing assay of CRC cells stably transfected with RSPO2 plasmid. The RSPO2 stable overexpression clone (R2) and a control clone with empty vector (Vec) were used for the experiments. (**E**) *Trans*-well migration and invasion assay of CRC cells stably transfected with RSPO2 plasmid. The error bars indicate the SD of three independent experiments. ***P < 0.001 vs. Vec. (**F-G**) RSPO2 inhibits CRC cell metastasis *in vivo*. SW480 cells stably transfected with RSPO2 (SW480-R2) plasmid or empty vector (SW480-Vec) were injected into the left ventricle of nude mice. Images were captured at different time points after injection. The photon counts of each animal are indicated by the color scale. The mean photon counts of each group of mice were quantified and are displayed over time. The error bars indicate the SD of the photon counts (n = 5). ***P < 0.001 vs. Vec. (**H**) Incidence (left panel) of liver metastatic tumors and H&E staining of metastatic nodules in the livers (right panel). (**A-H**) Mean ± SD; significance was determined using Student's *t*-test.

received cells stably overexpressing RSPO2. At the end of the experiments, metastatic liver nodules were observed in 40% of individual mice in the control group, but no metastatic nodules were observed in the RSPO2-overexpressing group (Fig. 1H). These findings were consistent with the *in vitro* results, indicating that RSPO2 exerted a suppressive effect on *in vitro* cell migration, invasion, and *in vivo* metastatic seeding.

RSPO2 suppresses EMT and MMP7/CD44 expression

EMT is a well-known mechanism involved in the invasion and metastasis of CRC tumors. To explore the mechanism in RSPO2-mediated cell migration, we first assessed the expression of epithelial and mesenchymal markers by western blotting. RSPO2 protein treatment increased the expression of the epithelial marker E-cadherin and decreased three mesenchymal markers (N-cadherin, vimentin, fibronectin) in SW480 and LOVO cells (Fig. 2A–B). These data suggested that RSPO2 had a negative influence on colon cancer cell EMT. To further investigate the molecular mechanisms by which RSPO2 suppressed the migration and invasion of CRC cells, we monitored the activities or expression levels of genes that are tightly associated with cancer metastasis (Fig. 2C, Supplementary Fig. 1C). Western blotting and immunofluorescence staining revealed that RSPO2 protein treatment or stable RSPO2 overexpression significantly down-regulated MMP7 protein expression in SW480 and LOVO cells compared with their controls (Fig. 2C–D, Supplementary Fig. 2A). In parallel, RSPO2 markedly decreased the CD44 protein levels in SW480 cells (CD44 expression in LOVO cells is undetectable) (Fig. 2C, Supplementary Fig. 2A–B). We then questioned whether the down-regulation of MMP7 and CD44 played a causal role in RSPO2-induced cancer cell migration and invasion. Stable MMP7 overexpression not only increased the invasiveness of cancer cells but also completely counteracted the RSPO2-mediated suppression of cellular migration and invasion (Fig. 2E, Supplementary Fig. 2C–D). These results indicated that MMP7 played a major role in RSPO2-induced cancer metastasis suppression. Stable CD44 overexpression promoted the migration of SW480 and LOVO cells, whereas CD44 knockdown by siRNA significantly inhibited the invasiveness of SW480 cells (Fig. 2F, Supplementary Fig. 3A). Knockdown of CD44 also abolished cell

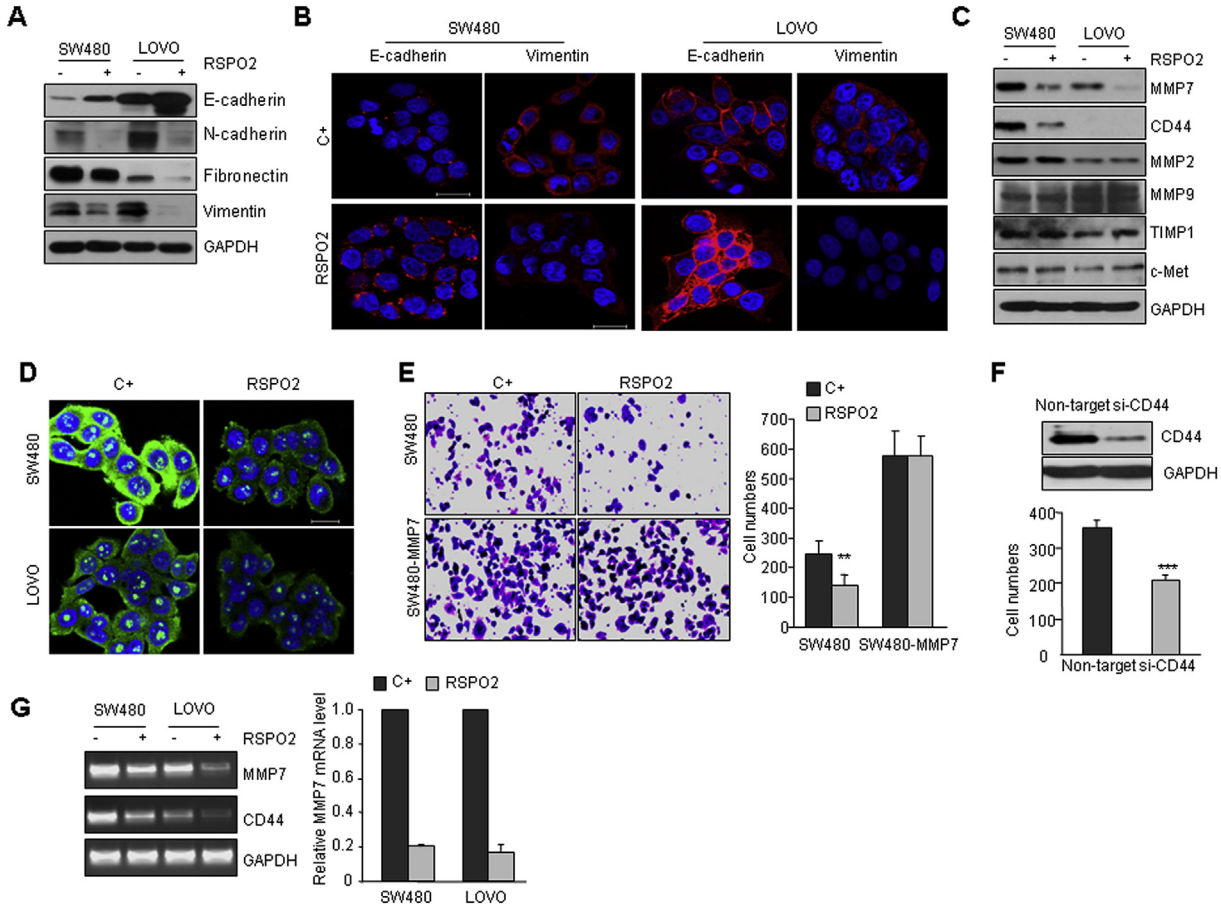

Fig. 2. RSPO2 suppresses CRC cell migration by inhibiting EMT and MMP7/CD44 expression. (**A**) Western blotting analysis of the epithelial marker E-cadherin and mesenchymal markers N-cadherin, vimentin, and fibronectin. Cells were treated with 100 ng/ml RSPO2 protein for 6 h. (**B**) Immunofluorescence staining of E-cadherin and vimentin protein expression after RSPO2 protein treatment. DAPI was used to visualize the nuclei. Scale bar, 20 μm. (**C**) Western blot analysis of migration-related gene expression after RSPO2 protein treatment. (**D**) Immunofluorescence staining of MMP7 protein expression after RSPO2 treatment. Scale bar, 20 μm. (**E**) *Trans*-well migration assay of SW480 and SW480 cells stably transfected with MMP7 plasmid (SW480-MMP7). MMP7 overexpression abolishes the inhibitory effect of RSPO2 on cell migration. The error bars indicate the SD of three independent experiments. $^{**}P < 0.01$ vs. C+. (**F**) *Trans*-well migration assay of SW480 cells after CD44 knockdown by siRNA. The error bars indicate the SD of three independent experiments. $^{***}P < 0.001$ vs. non-target. (**G**) The mRNA level of MMP7 and CD44 after RSPO2 protein treatment. Cells were treated with or without RSPO2 (100 ng/ml) for 6 h, and the mRNA level was detected by qRT-PCR. The data were calculated from triplicates. (**E-G**) Mean ± SD; significance was determined using Student's *t*-test.

migration induced by RSPO2 depletion (Supplementary Fig. 3B). These data suggested that CD44 partially contributed to RSPO2-induced cancer cell migratory suppression. In addition, real-time PCR demonstrated that RSPO2 protein treatment decreased MMP7 and CD44 mRNA expression levels, suggesting that RSPO2 inhibited the transcriptional activity of MMP7 and CD44 in CRC cells (Fig. 2G).

RSPO2 suppresses CRC tumor metastasis via the ERK-PEA3 cascade

Previously, we showed that RSPO2 inhibits CRC tumor proliferation through the canonical Wnt-β-catenin pathway [29]. MMP7 and CD44 are both targets of the Wnt-β-catenin signaling pathway. Therefore, we first examined whether this pathway was responsible for the RSPO2-induced metastasis suppression. However, we found that while RSPO2 enhanced β-catenin/TCF reporter activity in HEK293 cells, RSPO2 protein addition or knockdown of RSPO2 by siRNA did not have any effect on β-catenin/TCF reporter activity in SW480 or LOVO cells (Fig. 3A–B). Consistently, RSPO2 protein stimulation affected neither cytosolic/nuclear β-catenin nor β-catenin-dependent c-Myc expression (Fig. 3C, Supplementary Fig. 4A). Similar phenomena were observed in SW480 and LOVO clones that were stably transfected with an RSPO2 expression plasmid (Supplementary Fig. 4B–C). These results strongly suggested that RSPO2 suppressed CRC cell migration through mechanisms other than the inhibition of canonical Wnt/β-catenin signaling. Because mitogen-activated protein kinase (MAPK) cascades play critical roles in CRC cell mobility and metastasis, we next investigated the effects of RSPO2 on the JNK/ERK/P38 MAPK pathways. Preliminary data showed that RSPO2 did not affect the transcription of an AP-1-driven luciferase reporter gene (AP-1 Luc) (Fig. 3D), and western blotting confirmed that RSPO2 failed to suppress JNK and P38 phosphorylation (Fig. 3E). Interestingly, upon RSPO2 protein stimulation or stable RSPO2 overexpression, the level of phosphorylated ERK was markedly decreased in both SW480 and LOVO cells (Fig. 3E, Supplementary Fig. 5A). Pretreatment with the MEK inhibitor U0126 significantly reduced MMP-7 protein expression and correspondingly suppressed cancer cell migration (Fig. 3F). These results suggested that ERK signaling was responsible for RSPO2-induced cancer metastasis suppression in CRC tumors. Because c-Fos was difficult to detect in both cell lines (Supplementary Fig. 5B), we examined PEA3, another gene known to be downstream of the ERK cascade that may regulate MMP7 and CD44 expression [30,31]. We found that RSPO2 decreased the expression of PEA3 in SW480 and LOVO cells (Fig. 3E). PEA3 knockdown by siRNA down-regulated MMP7 and CD44 and correspondingly inhibited cancer

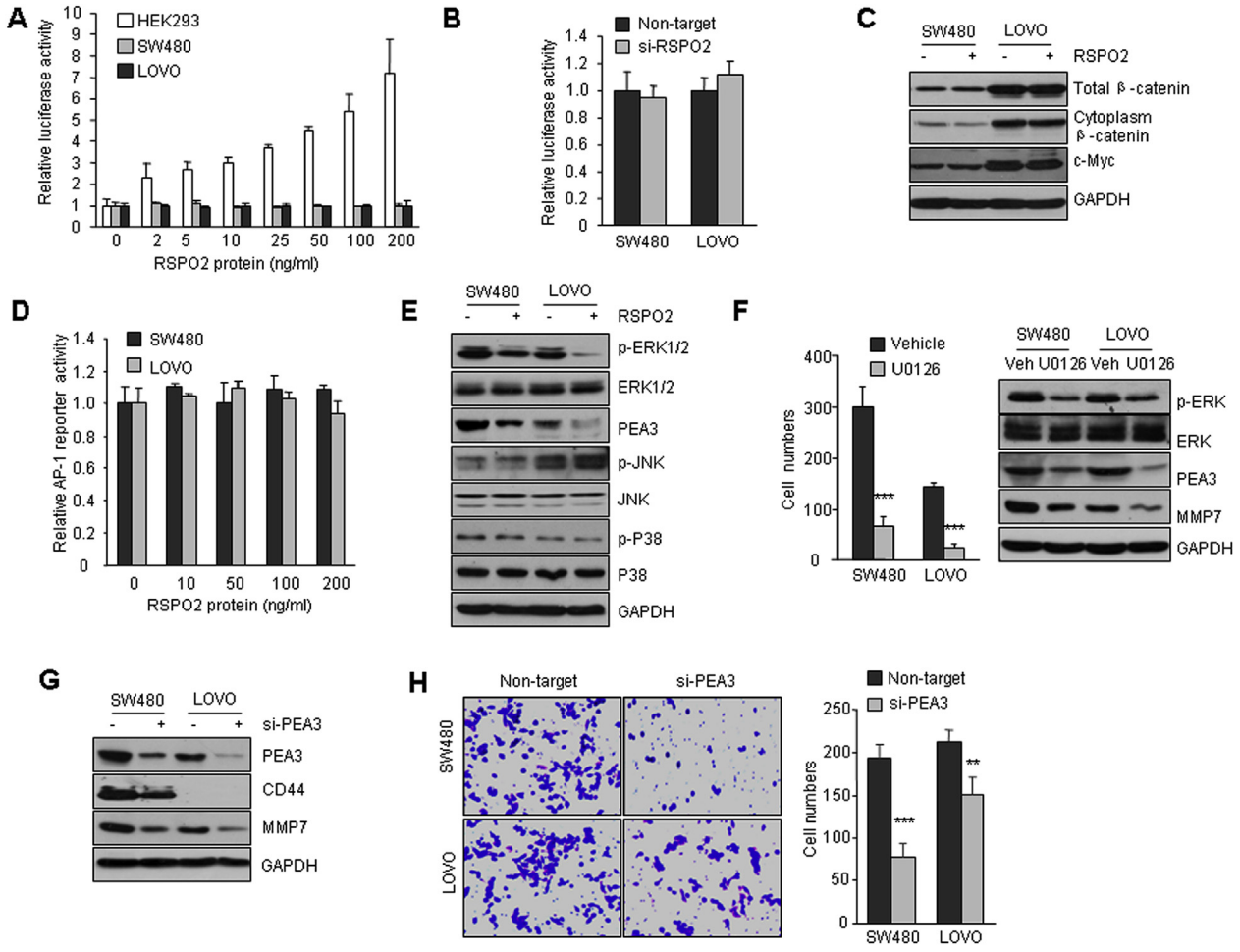

Fig. 3. RSPO2 suppresses CRC tumor metastasis through the ERK-PEA3 cascade. (**A**) β-catenin reporter assay in cells treated with recombinant RSPO2 protein (0–200 ng/ml). The data were calculated from triplicates. (**B**) β-catenin reporter assay in CRC cells after siRNA-mediated RSPO2 knockdown. The data were calculated from triplicates. (**C**) Effects of RSPO2 protein exposure on c-Myc and β-catenin accumulation. Cells were treated with 100 ng/ml RSPO2 protein for 6 h. (**D**) AP1 reporter assay in CRC cells after RSPO2 protein (0–200 ng/ml) treatment. (**E**) Effects of RSPO2 treatment on different MAPK pathway activation. Cells were treated with 100 ng/ml RSPO2 protein for 6 h. (**F**) Effects of MEK inhibitor U0126 treatment on ERK pathway activation and cell migration (cells were treated with 10 μM U0126 for 24 h). Error bars indicate the SD of three independent experiments. ***$P < 0.001$ vs. vehicle (DMSO). (**G**) PEA3 knockdown decreases MMP7 and CD44 expression. Non-target siRNA was used as a control. (**H**) *Trans*-well migration assay of CRC cells after PEA3 knockdown. Error bars indicate the SD of three independent experiments. **$P < 0.01$ vs. non-target. ***$P < 0.001$ vs. non-target. (**F, H**) Mean ± SD; significance was determined using Student's *t*-test.

cell migration (Fig. 3G–H). Taken together, these findings suggest that the ERK pathway plays a causal role in RSPO2-induced CRC metastasis suppression. RSPO2-induced ERK signaling inactivation decreased PEA3 expression, which subsequently suppressed MMP7/CD44 transcription and cancer cell migration.

RSPO2 suppresses the Fzd7-mediated noncanonical Wnt signaling pathway

The ERK pathway is primarily regulated by EGFR activation, which subsequently affects Ras activity. Although the phosphorylation of EGFR was attenuated in SW480 cells after exogenous RSPO2 protein exposure, no difference was observed in Ras activation (Fig. 4A). Inhibition by the EGFR family kinase inhibitor Cetuximab had no observable effect on cell migration at reasonable drug concentrations (Supplementary Fig. 6). This result suggested that RSPO2 might cross-regulate EGFR activation, but EGFR signaling was not responsible for the migration suppression in these two CRC cell lines. Because R-spondins have also been considered potential regulators in noncanonical Wnt signaling, we investigated the effects of RSPO2 on Fzd2 and Fzd7, two representative noncanonical Wnt receptors. RSPO2 protein treatment and stable RSPO2 overexpression both significantly decreased the levels of total and cell surface Fzd7 and, accordingly, the levels of phosphorylated-PKC/ERK (Fig. 4B–D, Supplementary Fig. 7A). No differences were observed in Fzd2 levels in the same experiment (Fig. 4B and D). Among the four recombinant human R-spondin proteins we examined, only RSPO2 showed a suppression effect on Fzd7 levels in both CRC cell lines (Supplementary Fig. 7B). To determine whether Fzd7 signaling was required for cell migration and whether RSPO2-Fzd7 signaling regulated CRC cell metastasis, we depleted or overexpressed Fzd7 in SW480 and LOVO cells. A significant reduction in cell migration was observed in Fzd7-depleted cells compared with control cells (Fig. 4E). Fzd7 overexpression completely abolished the RSPO2-mediated inhibition of cancer cell migration (Fig. 4F). These results suggested that Fzd7 played a causal role in RSPO2-induced cancer metastasis suppression. Fzd7 knockdown by siRNA decreased the levels of PKC and ERK phosphorylation, whereas ectopic Fzd7 overexpression enhanced PKC and ERK phosphorylation in both cell lines (Fig. 4G–H). These data suggested that RSPO2-induced PKC/ERK signaling inactivation was

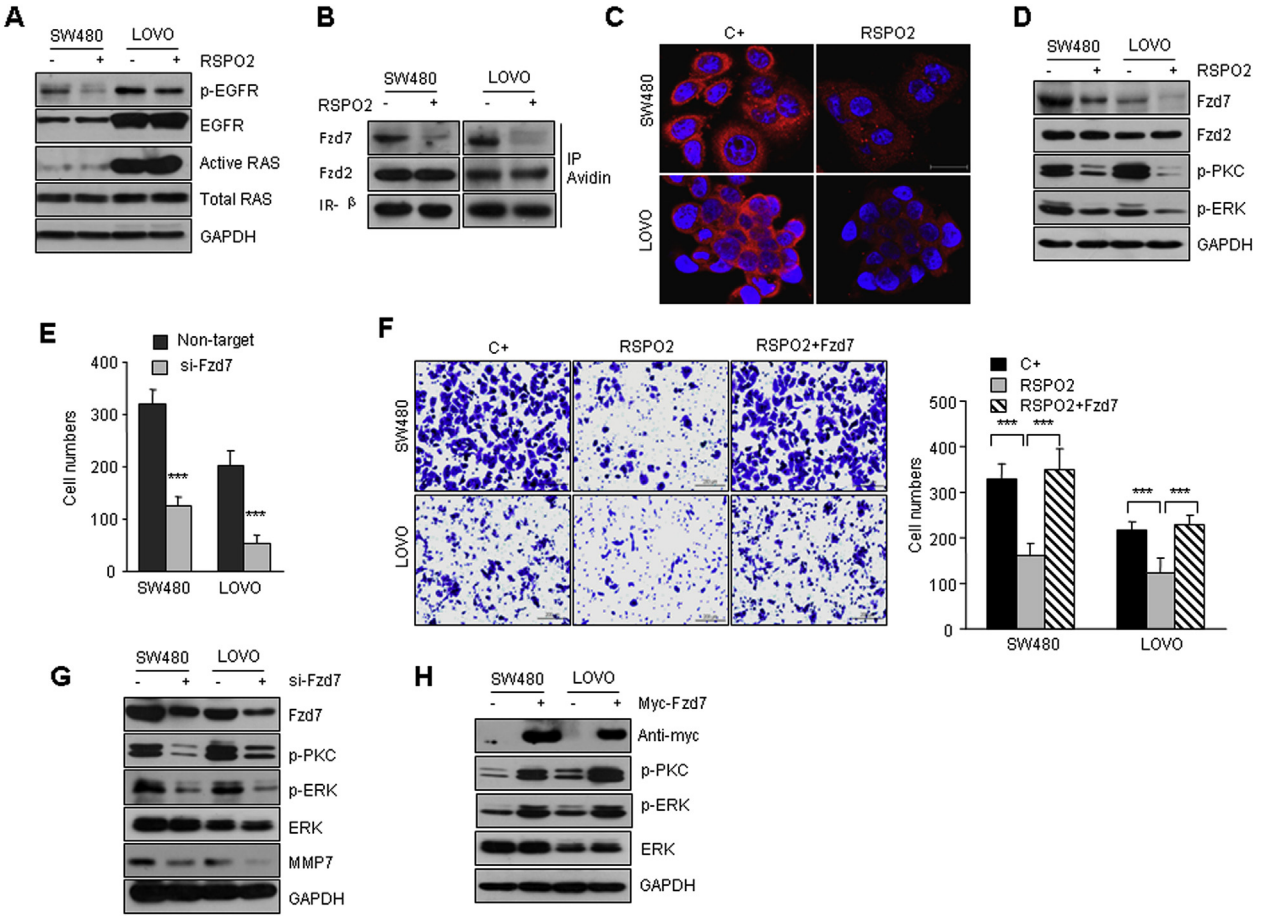

Fig. 4. RSPO2 suppresses noncanonical Fzd7/PKC signaling. (**A**) Effects of RSPO2 protein exposure on EGFR/Ras activation. Cells were stimulated with 100 ng/ml RSPO2 for 6 h. (**B**) Effects of RSPO2 protein treatment on cell surface Fzd2/7 accumulation. Cells were stimulated with 100 ng/ml RSPO2 for 6 h, and membrane protein (avidin pull-down) were probed by western blotting. Insulin receptor-β (IR-β) acts as a control. (**C**) Immunofluorescence staining of endogenous Fzd7 protein after RSPO2 stimulation. Scale bar, 20 μm. (**D**) RSPO2 exposure decreases Fzd7 accumulation and PKC/ERK phosphorylation. (**E**) *Trans*-well migration assays of CRC cells after Fzd7 knockdown. Non-target siRNA was used as a control. The error bars indicate the SD of three independent experiments. ***$P < 0.001$ vs. non-target. (**F**) Fzd7 abolishes the inhibitory effect of RSPO2 on CRC cell migration. Cells were co-transfected with RSPO2 and/or Fzd7 expression plasmids. The data were calculated from triplicates. ***$P < 0.001$. Scale bar, 20 μm. (**G-H**) Effects of Fzd7 knockdown or overexpression on PKC/ERK phosphorylation. Cells were transfected with si-Fzd7 or Fzd7 expression plasmid (myc-tagged); non-target siRNA or pcDNA3.1 empty vector were used as controls, respectively. (**E-F**) Mean ± SD; significance was determined using Student's *t*-test.

mediated via the Fzd7 receptor. Taken together, these results indicate that RSPO2 suppresses CRC metastasis through an Fzd7-mediated noncanonical Wnt signaling pathway.

RSPO2 promotes Fzd7 degradation via ZNRF3-mediated ubiquitination

In our previous report [29], we demonstrated that RSPO2 interacts with LGR5 to stabilize the membrane-associated zinc and ring finger protein ZNRF3 and thus suppresses canonical Wnt/β-catenin signaling and CRC cell growth. Intriguingly, although RSPO2 increased the accumulation of ZNRF3 on the cell membrane (Fig. 5A–B), it did not have any effect on Wnt/β-catenin signaling activity in SW480 and LOVO cells (Fig. 3A–C). These results implied that a novel mechanism was responsible for the RSPO2-induced tumor metastasis suppression in these CRC cells. Thus, we manipulated the expression of ZNRF3 in SW480 and LOVO cells and found that depletion of ZNRF3 by siRNA enhanced the accumulation of Fzd7 and PKC/ERK phosphorylation (Fig. 5C). In contrast, enforced ZNRF3 overexpression decreased the Fzd7 levels and PKC/ERK phosphorylation (Fig. 5D). These results indicated that RSPO2-induced ZNRF3 accumulation played a pivotal role in the inactivation of noncanonical Wnt signaling and cancer cell migration. ZNRF3 is a transmembrane E3 ubiquitin ligase that specifically mediates multi-ubiquitination and the degradation of Frizzled receptors [15,32]. Moreover, RSPO2 treatment did not affect the Fzd7 mRNA expression level (Supplementary Fig. 7C), suggesting that Fzd7 modulation might occur at the protein level. Next, we tested whether RSPO2 could promote the degradation of Fzd7 via ZNRF3-mediated ubiquitination. ZNRF3 overexpression significantly increased the levels of ubiquitinated Fzd7, whereas ZNRF3 knockdown by siRNA markedly decreased the accumulation of ubiquitinated Fzd7 (Fig. 5E, Supplementary Fig. 7D). Treatment with the proteasome inhibitor MG132 partially blocked the ZNRF3-mediated Fzd7 degradation (Supplementary Fig. 7E). These data indicated that ZNRF3 promoted Fzd7 degradation by directly increasing its ubiquitination. RSPO2 treatment increased the accumulation of ZNRF3 on the cell membrane and simultaneously promoted the ubiquitin-mediated degradation of Fzd7 in CRC cells (Fig. 5A and E). Taken together, these results suggest that RSPO2 induces membrane accumulation of ZNRF3, which triggers the degradation of the Wnt receptor Fzd7 by ubiquitination.

R-spondins and ZNRF3 have been shown to interact with LGRs and form a complex [33,34]. The discovery of the interaction between ZNRF3 and Frizzled proteins led us to consider the possibility of an RSPO2/LGR5/ZNRF3/Fzd7 complex [32] that could regulate

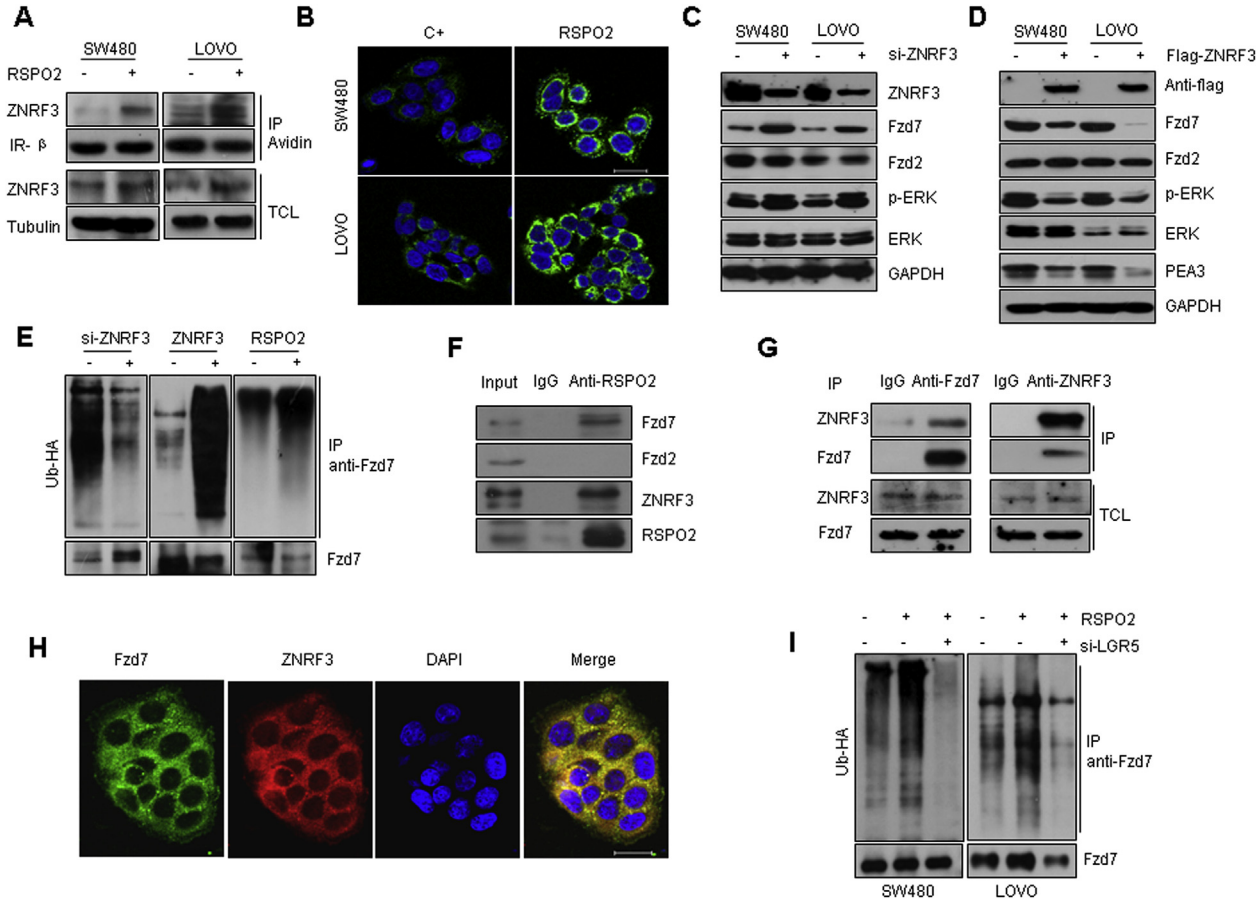

Fig. 5. RSPO2 promotes Fzd7 degradation via ZNRF3-mediated ubiquitination. (**A**) Effect of RSPO2 protein treatment on cell surface ZNRF3 accumulation. Cells were stimulated with 100 ng/ml RSPO2 for 6 h, and the total cell lysate (TCL) and membrane protein (avidin pull-down) were probed by western blotting. Insulin receptor-β (IR-β) acts as a control. (**B**) Immunofluorescence staining of endogenous ZNRF3 protein after RSPO2 stimulation. Scale bar, 20 μm. (**C-D**) Effects of ZNRF3 knockdown or overexpression on Fzd7 accumulation and ERK phosphorylation. Cells were transfected with si-ZNRF3 or ZNRF3 (Flag-tagged) expression plasmid; non-target siRNA or pcDNA3.1 empty vector were used as controls, respectively. (**E**) RSPO2 and ZNRF3 increase the ubiquitination (Ub-HA) of Fzd7. SW480 cells were transfected with si-ZNRF3 or ZNRF3 expression plasmid; non-target siRNA or pcDNA3.1 empty vector were used as controls, respectively. For RSPO2 treatment, the cells were stimulated with RSPO2 protein (100 ng/ml) for 6 h. (**F**) Co-immunoprecipitation of RSPO2 and endogenous ZNRF3/Fzd7. SW480 cells were transfected with RSPO2 expression plasmid. Immunoprecipitation was performed with anti-RSPO2, and immunoblotting was performed with the indicated antibodies. (**G**) Co-immunoprecipitation of Fzd7 and ZNRF3. SW480 cells were transfected with ZNRF3 expression plasmid. Immunoprecipitation was performed with either anti-Fzd7 or anti-ZNRF3. (**H**) Colocalization of ZNRF3 and Fzd7 in SW480 cells. Fzd7 and ZNRF3 were detected by immunofluorescence staining and confocal microscopy. Scale bar, 20 μm. (**I**) Effects of LGR5 knockdown on RSPO2-induced Fzd7 degradation.

Fzd7 degradation and noncanonical Wnt signaling. To test this possibility, the physical interactions between Fzd7 and RSPO2 or ZNRF3 were examined in SW480 cells by co-immunoprecipitation experiments. Ectopically expressed RSPO2 pulled down endogenous Fzd7 and ZNRF3 (Fig. 5F), and Fzd7 and ZNRF3 co-immunoprecipitated reciprocally (Fig. 5G). Moreover, a nearly complete colocalization of Fzd7 and ZNRF3 was observed in SW480 cells (Fig. 5H). These results suggested that RSPO2, ZNRF3, and Fzd7 were physically associated. Consistent with its incompetence in Wnt/β-catenin signaling activation, RSPO2 treatment did not have any effect on LGR5 mRNA expression in SW480 and LOVO cells (Supplementary Fig. 7F). However, knockdown of LGR5 significantly nullified the promoting effect of RSPO2 on Fzd7 degradation (Fig. 5I), suggesting that LGR5 was involved in RSPO2-mediated degradation of Fzd7 and that Fzd7 might be present in the RSPO2/LGR5/ZNRF3 complex.

RSPO2 antagonizes Wnt5a-induced noncanonical Wnt signal activation

Wnt5a is a representative ligand that activates the noncanonical Wnt signaling pathway. In our experiments with SW480 and LOVO cells, we found that Wnt5a promoted cancer cell migration and exhibited tumor metastasis-promoting activity (Fig. 6A). Fzd7 is the receptor for Wnt5a in noncanonical Wnt signaling activation. Therefore, we investigated whether Fzd7 signaling was required for cell migration induced by Wnt5a. Although Wnt5a showed no effect on canonical Wnt/β-catenin signaling activation in SW480 and LOVO cells (Fig. 6B, Supplementary Fig. 8A), Wnt5a treatment markedly increased Fzd7 levels and thus activated PKC and ERK phosphorylation in both cell lines (Fig. 6B). Notably, increased PKC and ERK activity also stimulated PEA3 and MMP7 expression in both CRC cell lines (Fig. 6B). Moreover, Wnt5a significantly decreased the ubiquitination and degradation of Fzd7 (Fig. 6C). Fzd7 knockdown completely abolished the activation of PKC/ERK phosphorylation induced by Wnt5a (Fig. 6D). These results indicated that Fzd7 was involved in Wnt5a-induced cell migration, and Wnt5a promoted PKC/ERK signaling activation by preventing the ubiquitin-mediated degradation of Fzd7. The observation that RSPO2 promoted Fzd7 degradation raised the possibility that RSPO2 and Wnt5a played opposing roles in CRC cell metastasis. We first examined whether RSPO2 could counteract the metastasis-promoting activities of Wnt5a. The concomitant addition of RSPO2 and Wnt5a proteins nullified the migration-promoting

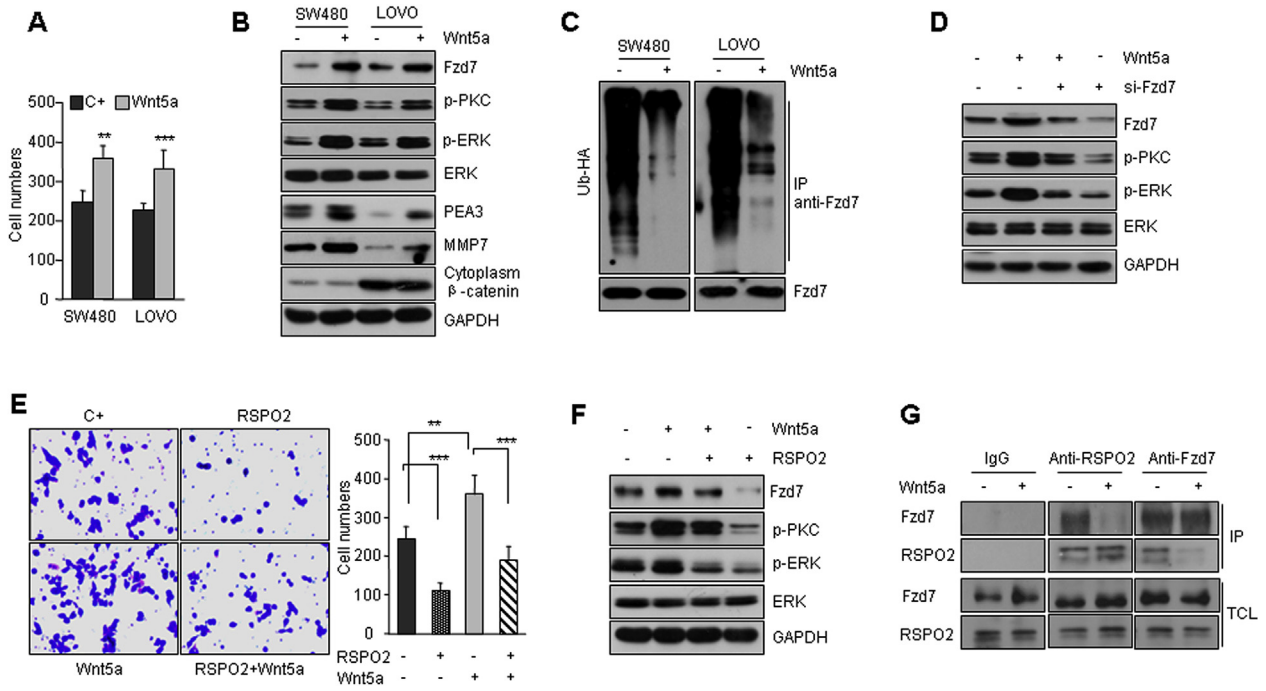

Fig. 6. RSPO2 antagonizes Wnt5a-induced noncanonical Wnt signal activation and cell migration. (**A**) *Trans*-well migration assays of CRC cells after Wnt5a treatment. Cells were pretreated with Wnt5a protein (100 ng/ml) for 6 h. The error bars indicate the SD of three independent experiments. **P < 0.01 vs. C+ (PBS); ***P < 0.001 vs. C+. (**B**) Effects of Wnt5a stimulation on noncanonical Fzd7 signaling activation. Cells were treated with Wnt5a (100 ng/ml) for 6 h, and cell lysates were analyzed with the indicated antibodies. (**C**) The levels of Fzd7 ubiquitination upon Wnt5a stimulation. Cells were treated with Wnt5a protein (100 ng/ml) for 6 h. (**D**) Effects of Fzd7 knockdown on Wnt5a-stimulated ERK activation. SW480 cells were treated with Wnt5a and/or transfected with Fzd7 siRNA, and cell lysates were analyzed with the indicated antibodies. (**E**) *Trans*-well migration assay of SW480 cells treated with RSPO2 and/or Wnt5a protein. The error bars indicate the SD of three independent experiments. **P < 0.01; ***P < 0.001. (**F**) Effects of RSPO2 protein treatment on Wnt5a-stimulated ERK activation. SW480 cells were treated with recombinant Wnt5a and/or RSPO2 protein. (**G**) Effects of Wnt5a on the interaction of RSPO2 with Fzd7 receptor. SW480 cells were transfected with RSPO2 and Fzd7 expression plasmids. PBS (−) or 500 μg/ml Wnt5a (+) protein was added to the cell lysates, and immunoprecipitation was performed with either anti-Fzd7 or anti-RSPO2 antibodies. (**A, E**) Mean ± SD; significance was determined using Student's *t*-test.

effect of Wnt5a in CRC cells treated with Wnt5a protein alone (Fig. 6E). Consistent with this phenotype, RSPO2 protein significantly attenuated Wnt5a-induced Fzd7 accumulation and PKC/ERK phosphorylation (Fig. 6F). Collectively, these results suggest that RSPO2 can antagonize Wnt5a-induced Fzd7/PKC/ERK signaling activation and consequently suppress CRC cell metastasis. To further investigate the mechanism involved in this process, additional co-immunoprecipitation studies were performed. As shown in Fig. 6G, in the presence of Wnt5a protein, the interaction between RSPO2 and Fzd7 was markedly blocked. These data suggest that Wnt5a can interfere with RSPO2 binding to Fzd7, thus antagonizing RSPO2-induced Fzd7 degradation.

Reduced RSPO2 expression is associated with poor survival

In our experiments with nine CRC cell lines, RSPO2 showed strong metastasis-suppressive activity only in SW480 and LOVO cells, two cell lines from late-stage CRC patients who express higher levels of Wnt5a (Supplementary Fig. 8B). These results implied that RSPO2 might preferentially suppress noncanonical Wnt signaling activation initiated by Wnt5a in late-stage CRC patients. When examining RSPO2 and Wnt5a expression in our CRC patient cohort by qRT-PCR, we found that low-level RSPO2 expression was associated with CRC tumor lymph node metastasis (Fig. 7A). Compared with the paired non-tumor tissues, RSPO2 mRNA expression was significantly reduced in the late-stage metastatic tumors, whereas Wnt5a mRNA expression was markedly up-regulated in the same subset of tumor tissues (Fig. 7A–B). A significant inverse correlation was detected between the mRNA levels of RSPO2 and Wnt5a in late-stage metastatic CRC tumors (Fig. 7C). These results suggested that RSPO2 and Wnt5a might play opposite roles in late-stage metastatic CRC patients. Metastasis is the major cause of cancer-related death. The association between low-level RSPO2 expression and tumor metastasis suggested that RSPO2 expression might be associated with CRC patient survival. To investigate the prognostic significance of RSPO2 in CRC patients, we mined the RSPO2 expression data in three CRC study datasets (GSE17536, GSE14333 and GSE17537). Kaplan-Meier analysis revealed that low-level RSPO2 expression was associated with poor overall survival and relapse-free survival in CRC patients (Fig. 7D–E, Supplementary Fig. 9). A significant association between high Wnt5a expression and poor survival was also found in the same GSE17536 cohort (Fig. 7F). Taken together, these data suggest that RSPO2 may play a critical role in Wnt5a-induced noncanonical Wnt signaling activation and CRC patient survival.

Discussion

Metastasis accounts for approximately 90% of the deaths of cancer patients [35]. Despite extensive research into the biology of cancer progression, the molecular mechanisms involved in CRC metastasis are not well characterized. The results of this study provide evidence that the RSPO2-mediated noncanonical Wnt signaling plays an important role in CRC metastasis. A novel mechanistic link between RSPO2 and Fzd7 was defined, in which RSPO2 induces Fzd7 degradation through E3 ligase ubiquitination of ZNRF3. The negative regulation of Fzd7 by RSPO2 inhibits PKC/ERK phosphorylation and downstream target gene transcription, thereby suppressing CRC tumor metastasis. Moreover, we found that Wnt5a promotes CRC cell migration through the same Fzd7/PKC/ERK signaling pathway, which

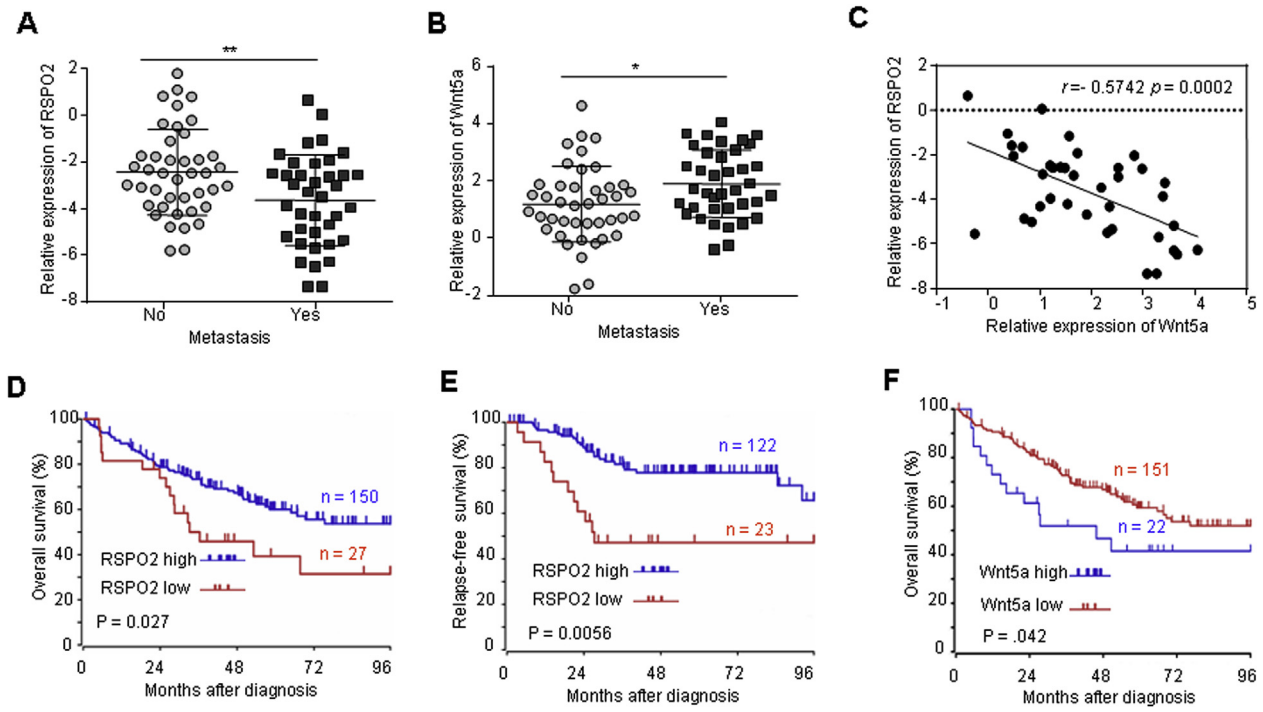

Fig. 7. Decreased RSPO2 expression is associated with metastasis and poor survival in CRC patients. (**A**) The expression levels of RSPO2 in CRC patients with and without metastasis. The mean level of RSPO2 expression in CRC patients with metastasis was significantly lower than that in CRC patients without metastasis. (Student's *t*-test, n = 80); **P < 0.01. (**B**) The expression of Wnt5a from the same CRC cohort. *P < 0.05. (**C**) Correlation analysis of RSPO2 and Wnt5a expression in late-stage metastatic CRC tumor samples. A negative correlation was detected between RSPO2 and Wnt5a expression (n = 38, Spearman P < 0.001). (**D-E**) Kaplan-Meier survival analysis of CRC patients with RSPO2-high vs. RSPO2-low tumors from the GSE17536 cohort. (**F**) Kaplan-Meier survival analysis of CRC patients with Wnt5a-high vs. Wnt5a-low tumors from the GSE17536 cohort. The censored values in Fig. 7D, E, and F were 49.7%, 68.2%, and 49.7%, respectively.

could be counteracted by RSPO2 protein. Combined with the clinical data analysis, we propose a novel RSPO2/Wnt5a-competing noncanonical Wnt signaling mechanism that contributes to the progression of metastatic CRC (Fig. 8).

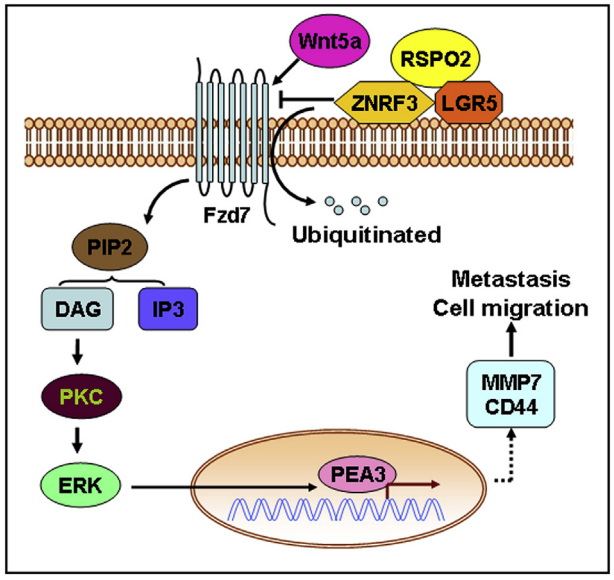

Fig. 8. Schematic of the RSPO2/Wnt5a-competing noncanonical Wnt signaling pathway. In late-stage CRC cells expressing high levels of Wnt5a, RSPO2 antagonizes the Wnt5a-driven noncanonical Wnt signaling by stabilizing membrane-associated ZNRF3, which triggers the ubiquitination and degradation of Fzd7 and thus attenuates the downstream PKC/ERK cascade that contributes to EMT, cellular migration, and tumor metastasis.

RSPO2 was first discovered as a Wnt/β-catenin signaling agonist and is commonly considered a potential proto-oncogene [24,36]. However, our previous study showed that RSPO2 inhibits CRC tumor growth through an LGR5-dependent Wnt/β-catenin signaling feedback loop [29]. In this study we demonstrated that RSPO2 suppresses human CRC metastasis. During the course of this study, Storm et al. reported that treatment with anti-RSPO2 antibody did not have an inhibitory effect on CRC tumor growth in a patient-derived xenograft (PDX) model [37]. These studies strengthen the conclusion that RSPO2 primarily functions as a tumor suppressor in human CRC. Intriguingly, the tumor metastasis-suppressive activity of RSPO2 is defined as being independent of the canonical Wnt/β-catenin pathway. RSPO2 suppressed CRC tumor metastasis through an Fzd7-mediated noncanonical Wnt signaling pathway. The well-recognized subcategories of noncanonical Wnt signaling are the Wnt/PCP pathway and the Wnt calcium signaling (Wnt/Ca^{2+}) pathway. In the Wnt/Ca^{2+} pathway, Wnt proteins activate intracellular Ca^{2+} signaling as well as Ca^{2+}-dependent protein kinases such as PKC and CAMKII [38]. In our experiments, RSPO2 suppressed the Fzd7-mediated PKC/ERK (but not the JNK/P38) pathway that led to PEA3 clearance. These results suggest that RSPO2 can specifically regulate an unconventional Wnt/Ca2+ signaling pathway in these CRC cells. PEA3 is a conserved ETS transcription factor that can regulate the expression of matrix metalloproteases (MMPs) during cancer metastasis [31,39]. Consistent with this regulation, we demonstrated that MMP7 plays a key role in RSPO2-induced CRC metastasis suppression. We also identified CD44 as a novel target gene that can be regulated by the RSPO2 and partially contribute to cancer cell migration; these results suggest that in addition to being a cancer stem cell marker, CD44 may play a role in CRC metastasis [40].

In this study, we have shown that RSPO2 promotes the degradation of Fzd7 via ZNRF3-mediated ubiquitination. ZNRF3 is a transmembrane E3 ubiquitin ligase that specifically mediates the multiubiquitination of Wnt receptors or coreceptors [15]. In HEK293 cells, a series of biochemical experiments has demonstrated that R-spondin can neutralize ZNRF3 on the plasma membrane and subsequently enhance canonical Wnt signaling activity [32]. However, in our previous study on two CRC cell lines, we demonstrated that RSPO2 could stabilize endogenous ZNRF3 on the cell membrane [29]. In this study, we observed a similar ZNRF3 accumulation in another two CRC cell lines after RSPO2 stimulation. A plausible explanation for these contrary results is that the functions of R-spondins may be dependent on the availability of LGR receptors and Wnt receptors/coreceptors. When LGR4 is present, RSPO1/3 induces the interaction between ZNRF3 and LGR4, which leads to the membrane clearance of ZNRF3 and the accumulation of Frizzled and LRP6, subsequently resulting in canonical Wnt/β-catenin signaling activation [41,42]. In the presence of IQGAP1, RSPO3-LGR4 functions via IQGAP1 to potentiate both the canonical and noncanonical Wnt signaling pathways [42]. In CRC tumors with high LGR5 receptor levels, RSPO2 has different functions from other R-spondin proteins. We have reported that RSPO2-LGR5 signaling promotes the clearance of LRP6, and subsequently suppresses Wnt/β-catenin signaling. In this study, we provide evidence that RSPO2 can suppress noncanonical Wnt signaling via Fzd7. Fzd7 is a representative noncanonical Wnt receptor that is overexpressed in colon cancer cells and late-stage CRC tumors [43]. Several studies have shown that Fzd7 is an oncogene involved in the survival, invasion, and metastasis of colon cancer cells [43,44]. Consistent with these studies, our results confirm that Fzd7 plays an oncogenic role in CRC tumor metastasis. Several molecular structures and mechanistic studies have demonstrated the presence of the RSPO/LGR/ZNRF3 complex [45]. In this study, specific interactions of Fzd7 with ZNRF3 and/or RSPO2 were observed. These results suggest that RSPO2 and Fzd7 may exist in the same LGR5/ZNRF3 complex and that the physical interaction between RSPO2 and Fzd7 is required for ZNRF3-mediated ubiquitination and degradation of Fzd7. Taken together, our findings suggest the presence of a previously unrecognized noncanonical Wnt signaling regulatory mechanism that is mediated through the RSPO2-LGR5/ZNRF3-Fzd7 axis and functions in CRC metastasis progression.

Wnt5a is a noncanonical Wnt protein that is involved in a broad range of cellular processes, particularly cancer development and metastasis [46]. However, the exact function of Wnt5a in cancer is controversial. Wnt5a acts as an oncogene in melanoma and breast cancer [47,48]. However, in other tumor models, including brain, hematopoietic tissue, and thyroid cancers, Wnt5a has been shown to inhibit tumor cell proliferation [49–51]. The role of Wnt5a in CRC appears to be more complex. Several studies have shown that Wnt5a acts as a tumor suppressor by inhibiting cell proliferation [52–54]. In this study, we demonstrated that Wnt5a exhibits a tumor metastasis-promoting effect in CRC cells. A plausible explanation for these paradoxical phenotypes is that the functions of Wnt5a may be dependent on the status of intrinsic canonical Wnt activity at different stages of tumor progression. Aberrant canonical Wnt/β-catenin activation functions principally in early stage carcinoma progression [55,56]. In accord with this pattern, tumor suppressor activity of Wnt5a was identified in HCT116 cells, a well-differentiated cell line that exhibits hyperactive Wnt/β-catenin activity [57]. Mechanistic studies revealed that Wnt5a overexpression provoked noncanonical Wnt/Ca^{2+} signaling, which subsequently antagonized canonical Wnt/β-catenin signaling in HCT116 cells [52,54]. In our experiments with late-stage CRC tumor cells, such as SW480 and LOVO, which have become unresponsive to canonical Wnt/β-catenin signaling stimulation [57,58], Wnt5a-mediated noncanonical Wnt signaling activation becomes the driving mechanism that promotes cancer aggressiveness. During the course of this study, Wnt5a was reported to promote metastasis in late-stage metastatic cancers via a Fzd2-mediated noncanonical pathway [59]; this finding is consistent with our results in CRC. In addition, we found that RSPO2 preferentially inhibits the migration of CRC cells with elevated Wnt5a expression. This phenomenon implies that the metastasis-suppressive function of RSPO2 may be dependent on the cellular context. In a subset of late-stage CRC tumor cells, RSPO2 can antagonize Wnt5a-driven noncanonical Wnt signaling activation and thereby suppress cancer cell migration. Intriguingly, we identified Fzd7 as the key mediator of both Wnt5a and RSPO2-mediated noncanonical Wnt signaling transduction during CRC tumor metastasis progression. Our data imply that competition exists between RSPO2 and Wnt5a in maintaining the stabilization of Fzd7 on the cell membrane. One possibility for the competition mechanism is that RSPO2 stabilizes cell surface ZNRF3, and simultaneously, RSPO2 competes with Wnt5a for binding to the Fzd7 receptor and thereby promotes the ubiquitin-mediated degradation of Fzd7. In late-stage metastatic CRC tumors, the absence of RSPO2 and an elevation of Wnt5a would be beneficial for the Fzd7-mediated noncanonical Wnt signaling activation and tumor metastasis, which is precisely the outcome we observed.

In summary, we found that RSPO2 has an inhibitory effect on CRC tumor cell migration and metastasis. The metastasis-suppressive activity of RSPO2 is dependent on the Fzd7-mediated noncanonical Wnt signal pathway. RSPO2 enhances the degradation of Fzd7 via ZNRF3-mediated ubiquitination. Wnt5a promotes cancer cell migration by preventing the degradation of Fzd7. RSPO2 antagonized Wnt5a-driven noncanonical Wnt signaling activation and tumor cell migration by blocking the binding of Wnt5a to Fzd7 receptor. We revealed an RSPO2/Wnt5a-competing mechanism that regulates noncanonical Wnt signal and CRC metastasis, and our data suggest that secreted RSPO2 may be a promising therapy for Wnt5a/Fzd7-driven aggressive CRC tumors.

Author contributions

The first three authors contributed equally to this paper. Dong X, Liao W and Zhang L performed the main experiments and analyzed the data; Hu J, Lu L, Liang W, Ding C and Liu R partially contributed to the experiments presented in this manuscript; Tu X and Wang O collected the clinical samples; Chen T, Dai X, Dai J and Xiong Y provided technical assistances; Liao W provided manuscript writing assistance; and Lu X conceived the study, designed the experiments, and wrote and finalized the manuscript.

Acknowledgments

We thank Véronique Orian-Rousseau at the Karlsruhe Institute of Technology for the CD44s expression plasmid. We thank Karl Willert at the University of California for the Fzd7 expression plasmid. We also thank Li-Hua Wang at the Eye Hospital of Wenzhou Medical University for technical assistance. This work was supported by the National Natural Science Foundation of China (No. 81572826 and 81372490), Zhejiang Provincial Natural Science Foundation (No. LZ14H160003) and Zhejiang Provincial Program for the Cultivation of High-Level Innovative Health Talents to Lu X. This work was also supported in part by the National Natural Science Foundation of China (No. 81472556 to Liao W; and No. 81501978 to Lu L) and Zhejiang Public Welfare Technologies Research (No. 2014C33257 to Tu X).

Competing interests

The authors declare no competing financial interests.

Appendix A. Supplementary data

Supplementary data related to this article can be found at http://dx.doi.org/10.1016/j.canlet.2017.05.024.

References

[1] A. Jemal, R. Siegel, E. Ward, Y. Hao, J. Xu, T. Murray, et al., Cancer statistics, 2008, CA Cancer J. Clin. 58 (2008) 71–96.
[2] L.A. Mina, G.W. Sledge Jr., Rethinking the metastatic cascade as a therapeutic target, Nat. Rev. Clin. Oncol. 8 (2011) 325–332.
[3] D. Hanahan, R.A. Weinberg, Hallmarks of cancer: the next generation, Cell 144 (2011) 646–674.
[4] T. Valenta, G. Hausmann, K. Basler, The many faces and functions of beta-catenin, EMBO J. 31 (2012) 2714–2736.
[5] D.H. Kho, J.A. Bae, J.H. Lee, H.J. Cho, S.H. Cho, J.H. Lee, et al., KITENIN recruits Dishevelled/PKC delta to form a functional complex and controls the migration and invasiveness of colorectal cancer cells, Gut 58 (2009) 509–519.
[6] S.K. Dissanayake, M. Wade, C.E. Johnson, M.P. O'Connell, P.D. Leotlela, A.D. French, et al., The Wnt5A/protein kinase C pathway mediates motility in melanoma cells via the inhibition of metastasis suppressors and initiation of an epithelial to mesenchymal transition, J. Biol. Chem. 282 (2007) 17259–17271.
[7] J.K. Yoon, J.S. Lee, Cellular signaling and biological functions of R-spondins, Cell Signal 24 (2012) 369–377.
[8] W.B. de Lau, B. Snel, H.C. Clevers, The R-spondin protein family, Genome Biol. 13 (2012) 242.
[9] K.A. Kim, M. Kakitani, J. Zhao, T. Oshima, T. Tang, M. Binnerts, et al., Mitogenic influence of human R-spondin1 on the intestinal epithelium, Science 309 (2005) 1256–1259.
[10] B. Capel, R-spondin1 tips the balance in sex determination, Nat. Genet. 38 (2006) 1233–1234.
[11] M. Aoki, M. Mieda, T. Ikeda, Y. Hamada, H. Nakamura, H. Okamoto, R-spondin3 is required for mouse placental development, Dev. Biol. 301 (2007) 218–226.
[12] M.N. Knight, K.D. Hankenson, R-spondins: novel matricellular regulators of the skeleton, Matrix Biol. 37C (2014) 157–161.
[13] L.W. de, N. Barker, T.Y. Low, B.K. Koo, V.S. Li, H. Teunissen, et al., Lgr5 homologues associate with Wnt receptors and mediate R-spondin signalling, Nature 476 (2011) 293–297.
[14] K.S. Carmon, X. Gong, Q. Lin, A. Thomas, Q. Liu, R-spondins function as ligands of the orphan receptors LGR4 and LGR5 to regulate Wnt/beta-catenin signaling, Proc. Natl. Acad. Sci. U. S. A. 108 (2011) 11452–11457.
[15] L.W. de, W.C. Peng, P. Gros, H. Clevers, The R-spondin/Lgr5/Rnf43 module: regulator of Wnt signal strength, Genes Dev. 28 (2014) 305–316.
[16] B. Ohkawara, A. Glinka, C. Niehrs, Rspo3 binds syndecan 4 and induces Wnt/PCP signaling via clathrin-mediated endocytosis to promote morphogenesis, Dev. Cell 20 (2011) 303–314.
[17] B. Scholz, C. Korn, J. Wojtarowicz, C. Mogler, I. Augustin, M. Boutros, et al., Endothelial RSPO3 controls vascular stability and pruning through non-canonical WNT/Ca(2+)/NFAT signaling, Dev. Cell 36 (2016) 79–93.
[18] A. Glinka, C. Dolde, N. Kirsch, Y.L. Huang, O. Kazanskaya, D. Ingelfinger, et al., LGR4 and LGR5 are R-spondin receptors mediating Wnt/beta-catenin and Wnt/PCP signalling, EMBO Rep. 12 (2011) 1055–1061.
[19] V. Theodorou, M.A. Kimm, M. Boer, L. Wessels, W. Theelen, J. Jonkers, et al., MMTV insertional mutagenesis identifies genes, gene families and pathways involved in mammary cancer, Nat. Genet. 39 (2007) 759–769.
[20] M. Klauzinska, B. Baljinnyam, A. Raafat, J. Rodriguez-Canales, L. Strizzi, Y.E. Greer, et al., Rspo2/Int7 regulates invasiveness and tumorigenic properties of mammary epithelial cells, J. Cell Physiol. 227 (2012) 1960–1971.
[21] T.K. Starr, R. Allaei, K.A. Silverstein, R.A. Staggs, A.L. Sarver, T.L. Bergemann, et al., A transposon-based genetic screen in mice identifies genes altered in colorectal cancer, Science 323 (2009) 1747–1750.
[22] A.L. Watson, E.P. Rahrmann, B.S. Moriarity, K. Choi, C.B. Conboy, A.D. Greeley, et al., Canonical Wnt/beta-catenin signaling drives human schwann cell transformation, progression, and tumor maintenance, Cancer Discov. 3 (2013) 674–689.
[23] D. Robinson, E.M. Van Allen, Y.M. Wu, N. Schultz, R.J. Lonigro, J.M. Mosquera, et al., Integrative clinical genomics of advanced prostate cancer, Cell. 161 (2015) 1215–1228.
[24] S. Seshagiri, E.W. Stawiski, S. Durinck, Z. Modrusan, E.E. Storm, C.B. Conboy, et al., Recurrent R-spondin fusions in colon cancer, Nature 488 (2012) 660–664.
[25] J. Hilkens, N.C. Timmer, M. Boer, G.J. Ikink, M. Schewe, A. Sacchetti, et al., RSPO3 expands intestinal stem cell and niche compartments and drives tumorigenesis, Gut 66 (6) (2017) 1095–1105.
[26] X. Gong, J. Yi, K.S. Carmon, C.A. Crumbley, W. Xiong, A. Thomas, et al., Aberrant RSPO3-LGR4 signaling in Keap1-deficient lung adenocarcinomas promotes tumor aggressiveness, Oncogene 34 (2015) 4692–4701.
[27] P. Parma, O. Radi, V. Vidal, M.C. Chaboissier, E. Dellambra, S. Valentini, et al., R-spondin1 is essential in sex determination, skin differentiation and malignancy, Nat. Genet. 38 (2006) 1304–1309.
[28] S.Q. Kuang, W.G. Tong, H. Yang, W. Lin, M.K. Lee, Z.H. Fang, et al., Genome-wide identification of aberrantly methylated promoter associated CpG islands in acute lymphocytic leukemia, Leukemia 22 (2008) 1529–1538.
[29] C. Wu, S. Qiu, L. Lu, J. Zou, W.F. Li, O. Wang, et al., RSPO2-LGR5 signaling has tumour-suppressive activity in colorectal cancer, Nat. Commun. 5 (2014) 3149.
[30] R.C. O'Hagan, R.G. Tozer, M. Symons, F. McCormick, J.A. Hassell, The activity of the Ets transcription factor PEA3 is regulated by two distinct MAPK cascades, Oncogene 19 (13) (1996) 1323–1333.
[31] L.Y. de, J.L. Baert, A. Chotteau-Lelievre, D. Monte, L. Coutte, S. Mauen, et al., The Ets transcription factors of the PEA3 group: transcriptional regulators in metastasis, Biochim. Biophys. Acta 1766 (2006) 79–87.
[32] H.X. Hao, Y. Xie, Y. Zhang, O. Charlat, E. Oster, M. Avello, et al., ZNRF3 promotes Wnt receptor turnover in an R-spondin-sensitive manner, Nature 485 (2012) 195–200.
[33] M. Zebisch, Y. Xu, C. Krastev, B.T. MacDonald, M. Chen, R.J. Gilbert, et al., Structural and molecular basis of ZNRF3/RNF43 transmembrane ubiquitin ligase inhibition by the Wnt agonist R-spondin, Nat. Commun. 4 (2013) 2787, http://dx.doi.org/10.1038/ncomms3787.
[34] D. Wang, B. Huang, S. Zhang, X. Yu, W. Wu, X. Wang, Structural basis for R-spondin recognition by LGR4/5/6 receptors, Genes Dev. 27 (2013) 1339–1344.
[35] S. Valastyan, R.A. Weinberg, Tumor metastasis: molecular insights and evolving paradigms, Cell 147 (2011) 275–292.
[36] O. Kazanskaya, A. Glinka, B.B. del I, P. Stannek, C. Niehrs, W. Wu, R-Spondin2 is a secreted activator of Wnt/beta-catenin signaling and is required for Xenopus myogenesis, Dev. Cell 7 (2004) 525–534.
[37] E.E. Storm, S. Durinck, e Melo de Sousa, J. Tremayne, N. Kljavin, C. Tan, et al., Targeting PTPRK-RSPO3 colon tumours promotes differentiation and loss of stem-cell function, Nature 529 (2016) 97–100.
[38] C. Niehrs, The complex world of WNT receptor signalling, Nat. Rev. Mol. Cell Biol. 13 (2012) 767–779.
[39] C.C. Lynch, H.C. Crawford, L.M. Matrisian, S. McDonnell, Epidermal growth factor upregulates matrix metalloproteinase-7 expression through activation of PEA3 transcription factors, Int. J. Oncol. 24 (2004) 1565–1572.
[40] P. Dalerba, S.J. Dylla, I.K. Park, R. Liu, X. Wang, R.W. Cho, et al., Phenotypic characterization of human colorectal cancer stem cells, Proc. Natl. Acad. Sci. U. S. A. 104 (2007) 10158–10163.
[41] Y. Xie, R. Zamponi, O. Charlat, M. Ramones, S. Swalley, X. Jiang, et al., Interaction with both ZNRF3 and LGR4 is required for the signalling activity of R-spondin, EMBO Rep. 14 (2013) 1120–1126.
[42] K.S. Carmon, X. Gong, J. Yi, A. Thomas, Q. Liu, RSPO-LGR4 functions via IQGAP1 to potentiate Wnt signaling, Proc. Natl. Acad. Sci. U. S. A. 111 (2014) E1221–E1229.
[43] T.D. King, W. Zhang, M.J. Suto, Y. Li, Frizzled7 as an emerging target for cancer therapy, Cell Signal 24 (2012) 846–851.
[44] K. Ueno, S. Hazama, S. Mitomori, M. Nishioka, Y. Suehiro, H. Hirata, et al., Down-regulation of frizzled-7 expression decreases survival, invasion and metastatic capabilities of colon cancer cells, Br. J. Cancer. %20 101 (2009) 1374–1381.
[45] M. Zebisch, E.Y. Jones, Crystal structure of R-spondin 2 in complex with the ectodomains of its receptors LGR5 and ZNRF3, J. Struct. Biol. 191 (2015) 149–155.
[46] N. Zhu, L. Qin, Z. Luo, Q. Guo, L. Yang, D. Liao, Challenging role of Wnt5a and its signaling pathway in cancer metastasis (Review), Exp. Ther. Med. 8 (2014) 3–8.
[47] T. Pukrop, F. Klemm, T. Hagemann, D. Gradl, M. Schulz, S. Siemes, et al., Wnt 5a signaling is critical for macrophage-induced invasion of breast cancer cell lines, Proc. Natl. Acad. Sci. U. S. A. 103 (2006) 5454–5459.
[48] A.T. Weeraratna, Y. Jiang, G. Hostetter, K. Rosenblatt, P. Duray, M. Bittner, et al., Wnt5a signaling directly affects cell motility and invasion of metastatic melanoma, Cancer Cell. 1 (2002) 279–288.
[49] H. Liang, Q. Chen, A.H. Coles, S.J. Anderson, G. Pihan, A. Bradley, et al., Wnt5a inhibits B cell proliferation and functions as a tumor suppressor in hematopoietic tissue, Cancer Cell. 4 (2003) 349–360.
[50] N. Kremenevskaja, W.R. von, A.S. Rao, C. Schofl, T. Andersson, G. Brabant, Wnt-5a has tumor suppressor activity in thyroid carcinoma, Oncogene 24 (2005) 2144–2154.
[51] J.M. Yu, E.S. Jun, J.S. Jung, S.Y. Suh, J.Y. Han, J.Y. Kim, et al., Role of Wnt5a in the proliferation of human glioblastoma cells, Cancer Lett. 257 (2007) 172–181.
[52] J. Ying, H. Li, J. Yu, K.M. Ng, F.F. Poon, S.C. Wong, et al., WNT5A exhibits tumor-suppressive activity through antagonizing the Wnt/beta-catenin signaling, and is frequently methylated in colorectal cancer, Clin. Cancer Res. 14 (2008) 55–61.
[53] J. Dejmek, A. Dejmek, A. Safholm, A. Sjolander, T. Andersson, Wnt-5a protein expression in primary dukes B colon cancers identifies a subgroup of patients with good prognosis, Cancer Res. 65 (2005) 9142–9146.
[54] R. Cheng, B. Sun, Z. Liu, X. Zhao, L. Qi, Y. Li, et al., Wnt5a suppresses colon cancer by inhibiting cell proliferation and epithelial-mesenchymal transition, J. Cell Physiol. 229 (2014) 1908–1917.
[55] A. Walther, E. Johnstone, C. Swanton, R. Midgley, I. Tomlinson, D. Kerr, Genetic prognostic and predictive markers in colorectal cancer, Nat. Rev. Cancer 9 (2009) 489–499.

[56] R.H. Giles, J.H. van Es, H. Clevers, Caught up in a Wnt storm: Wnt signaling in cancer, Biochim. Biophys. Acta 1653 (2003) 1–24.
[57] E. Lavergne, I. Hendaoui, C. Coulouarn, C. Ribault, J. Leseur, P.A. Eliat, et al., Blocking Wnt signaling by SFRP-like molecules inhibits in vivo cell proliferation and tumor growth in cells carrying active beta-catenin, Oncogene 30 (2011) 423–433.
[58] M. Yashiro, K. Hirakawa, C.R. Boland, Mutations in TGFbeta-RII and BAX mediate tumor progression in the later stages of colorectal cancer with microsatellite instability, BMC. Cancer 10 (2010) 303–310, http://dx.doi.org/10.1186/1471-2407-10-303.
[59] T.S. Gujral, M. Chan, L. Peshkin, P.K. Sorger, M.W. Kirschner, G. MacBeath, A noncanonical Frizzled2 pathway regulates epithelial-mesenchymal transition and metastasis, Cell 159 (2014) 844–856.